Review on Impact Response of Reinforced Concrete Beams: Contemporary Understanding and Unsolved Problems

Thong M. Pham[1], Wensu Chen[2] and Hong Hao[3]

Abstract

Designing protective reinforced concrete (RC) beams against impact loadings is a challenging task. It requires a comprehensive understanding of the structural response of RC beams subjected to impact loads. Significant research efforts have been spent to unveil the impact response of RC beams by using analytical models, experimental testing, or numerical investigations. However, these studies used various assumptions in the analytical derivations and different test setups in the impact testing, which led to significantly different responses and observations of similar structures and similar loading conditions. For example, a minor change in contact surface can triple the maximum impact force of identical RC beams. This study provides a review of the contemporary understandings of the RC beam responses to impact loads, and explains the different observations and conclusions. Some unsolved issues for protective structures, i.e. RC beams to resist impulsive loads are also discussed. It is suggested that future studies should take into consideration the conditions of the test setup, simplifications and assumptions made in analytical derivations for better interpretations of the obtained results.

Keywords: Impact loading; analytical models; numerical simulation; contact mechanism; Protective structures; RC Beam.

---

[1] Senior Lecturer, Center for Infrastructural Monitoring and Protection, School of Civil and Mechanical Engineering, Curtin University, Kent Street, Bentley, WA 6102, Australia (corresponding author). Email: thong.pham@curtin.edu.au

[2] Senior Lecturer, Center for Infrastructural Monitoring and Protection, School of Civil and Mechanical Engineering, Curtin University, Kent Street, Bentley, WA 6102, Australia. Email: wensu.chen@curtin.edu.au

[3]John Curtin Distinguished Professor, Center for Infrastructural Monitoring and Protection, School of Civil and Mechanical Engineering, Curtin University, Kent Street, Bentley, WA 6102, Australia (corresponding author). Email: hong.hao@curtin.edu.au

Introduction

The dynamic response of beam elements has been investigated by many researchers due to design requirements for protective structures against impulsive loads. Earlier studies on the impact responses focused primarily on steel and composite beams rather than concrete beams by researchers in the field of mechanical engineering (Jones, 2011; Biggs, 1964; Abrate, 2005; Bangash, 2009; Johnson, 1972; Lu and Yu, 2003). The impact mechanisms of steel and composite beams have been well unveiled and documented in these books. However, directly applying the understandings of steel and composite beams to reinforced concrete (RC) beams is not necessarily appropriate due to their primary differences in material properties and response characteristics. For example, the shear strength of steel is comparable to its tensile strength, concrete is much stronger in compression than shear or tension, as a result, the shear failure dominance phenomenon was observed in RC beams subjected to impact loads and reported in previous experimental studies (Saatci and Vecchio, 2009; Pham and Hao, 2017b; Pham and Hao, 2016; Tran et al., 2021; Pham et al., 2021). This phenomenon was observed in RC beams having sufficient static shear strength but not necessarily sufficient dynamic shear resistance owing to the localized response of RC beams subjected to impact loads. The formation of the plastic hinge in RC beams is also different from that in steel beams due to the distinguished material properties of these two materials (Pham and Hao, 2017d).

Different approaches have been commonly adopted to study the impact response of protective structures, i.e. RC beams, including analytical, experimental, and numerical methods. For experimental investigations, the drop-weight apparatus has become the most popular technique for studying the impact response of RC beams (Yi et al., 2016; Saatci and Vecchio, 2009; Kishi et al., 2002a; Fujikake et al., 2009; Pham and Hao, 2017b; Pham and Hao, 2016; Hao and Pham, 2017). There are many different parameters and factors in the drop-weight tests which can significantly affect the impact response of RC beams but they were not clearly

discussed. For example, various impactor heads were used and they resulted in different responses although the drop weight and impact velocity are the same (Li et al., 2019a). The interlayer, which is placed between the impactor and the tested beam made of different materials such as steel and rubber obviously affects the impact response of RC beams. Also, the appearance and cause of the negative bending moment and negative reaction force recorded in impact tests of RC beams have not been carefully investigated and clearly explained either. For numerical studies, there have been quite a few studies investigating the impact response of RC beams (Kishi et al., 2011; Wu et al., 2016; Villavicencio and Guedes Soares, 2011; Jiang and Chorzepa, 2015; Anil et al., 2016; Adhikary et al., 2015; Ožbolt and Sharma, 2011; Luccioni et al., 2013b; Sharma and Ožbolt, 2014; Papadrakakis et al., 2016; Jiang et al., 2012), which used different numerical approaches and/or hydrocodes, such as LS-DYNA, AUTODYN, and ABAQUS. As a result, various contact mechanisms were utilized to model the impact between an impactor and a beam without appropriate justifications. Besides, different material models, erosion criteria, dynamic increase factors, etc. were used but their advantages and disadvantages and suitability have not been clearly discussed (Cui et al., 2017). Meanwhile, analytical models on the impact response of RC beams have also been proposed, in which various assumptions were made but their limitations have not been well addressed. All these variations may result in different understanding and observations for similar impact problems, which may further lead to misleading conclusions and recommendations. These issues require a comprehensive review and thorough discussions so that consensuses are made for understood phenomena while unsolved problems are raised for future research. This study, therefore, aims to provide a critical review of existing experimental, numerical, and analytical studies on the impact responses of RC beams.

Experimental impact tests

Under drop-weight tests, an impactor, which is usually made of steel, is raised to a designated height and dropped onto a target, i.e. concrete beam as shown in Fig. 1. The impactor goes into contact with the beam within a short period before their separation. The impactor and the beam may be in contact again depending on their interaction which may cause multiple peaks in the impact force-time history. During an impact event, the beam rebounds and is subjected to both uplift and downward responses. As a result, the beam supports need to be restrained at two sides including lower and upper surfaces as shown in Fig. 1. The impact force, reaction forces at the two sides and displacements should be also monitored. These forces are usually measured by load cells while there has been another method to estimate the impact force by using accelerometers and Newton's second law. Meanwhile, the beam displacement can be measured by either a high-speed camera together with an image processing technique or linear variable differential transformers (LVDT). All these sensors need to be used together with a high-speed acquisition system which has a sufficiently high sampling rate for properly recording signals. It is worth mentioning that the sampling rate of an acquisition system is of utmost importance since it significantly affects the recording data and thus analysis and following interpretations, which will be discussed in the subsequent section. In addition, the progressive failure of a beam can be monitored by using a high-speed camera with a sufficient frame rate. These measures and factors are essentially important to achieve accurate measures for impact tests and appropriate data interpretation. However, there have been many different ways of the test setup, equipment, and data processing in the open literature. The same test setup and identical specimens but only different sampling rates could lead to different measured data and thus interpretation and understanding. For example, Pham and Hao (2017a) adopted the same impact test setup for identical concrete cylinders and monitored the impact force-time histories. The maximum axial impact forces for identical cylinders under the same impact condition were 60 kN, 350 kN and 550 kN when sampling rate was set to be 20 kHz, 100 kHz and 1 MHz in the tests. The lack of standards and guidelines for this type of

test may lead to inaccurate results. The effects of these factors, therefore, are discussed in the subsequent sections.

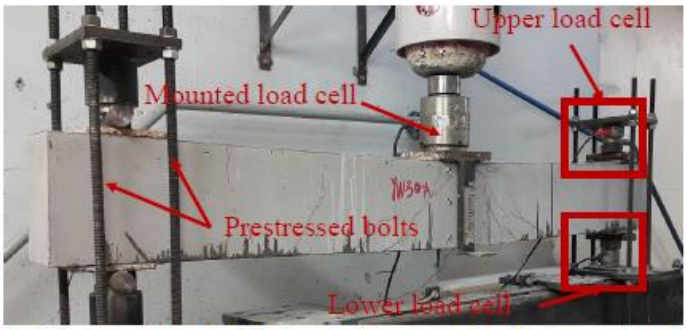

Load cell is mounted to an RC beam with two load cells for reaction forces

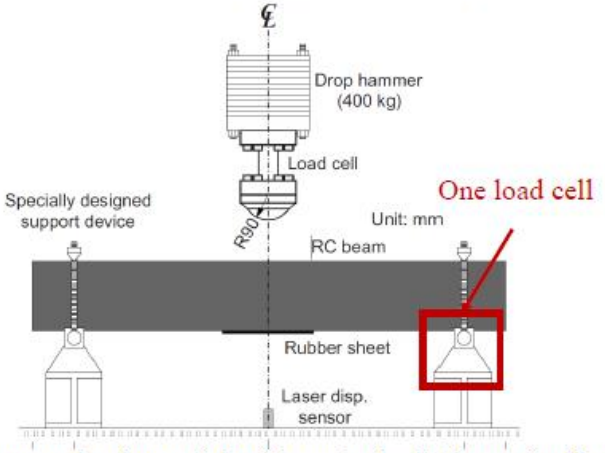

Load cell is mounted to drop-weight with one load cells for reaction forces
(Fujikake et al. 2009)

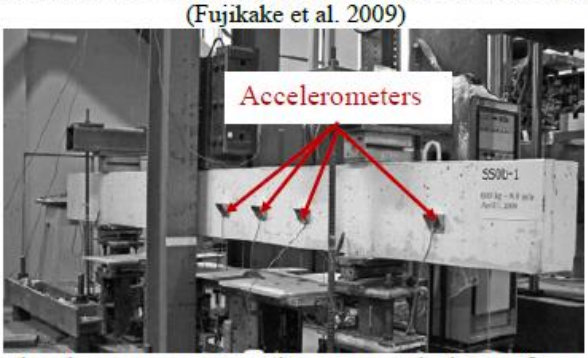

Accelerometers were used to compute the impact force
(Saatci and Vecchio 2009)

Fig. 1. Different methods of measuring impact forces and reaction forces

Impact force measurement

The impact force is an important measure to investigate the impact response of RC beams. The impact force is usually measured by direct or indirect methods in which the direct method

uses a load cell to record impact force. Meanwhile, the acceleration field of RC beams together with Newton's second law can also be utilized to quantify the beam's impact force. Acceleration is measured by accelerometers mounted along the longitudinal axis of the beam as shown in Fig. 1. The pros and cons of these two methods are discussed in detail in the following section.

One of the indirect methods to obtain impact force is to multiply the drop-weight mass by the acceleration, which can be measured by an accelerometer attached to the drop-weight (Kishi and Bhatti, 2010; Huynh et al., 2015; Yoo et al., 2015). Different accelerometers have different measurement ranges, therefore need be properly selected, e.g., accelerometers with frequency up to 7 kHz and amplitude up to 1000 g were selected in impact tests in (Kishi and Bhatti, 2010). On the other hand, the acceleration can be also obtained by differentiating the impact velocity of drop-weight measured by a laser Doppler velocimetry (LDV) system (Al-Rifaie et al., 2017; Al-Rifaie et al., 2018). Another indirect method to obtain the impact force is to sum up the reaction force at the supports and the integration of the acceleration and mass along the beam length (Huynh et al., 2015; Saatci and Vecchio, 2009). It should be noted that the abovementioned indirect methods to quantify impact force primarily depend on the measurement accuracy of acceleration and velocity. An insufficient sampling rate of the accelerometer (e.g. 7 kHz) might miss the peak of impact force and significant oscillation of the acceleration measurements could result in unreliable impact force estimations.

On the other hand, the direct method to measure impact force has been used in most impact tests (Zhao et al., 2017b; Tachibana et al., 2010; Fujikake et al., 2009; Kishi et al., 2002b; Pham et al., 2018; Yan et al., 2018). The impact force is recorded by load cells, which can be either strain gauge type (Isaac et al., 2017; Yoo and Banthia, 2017; Dey et al., 2014) or piezoelectric type (Wang et al., 2019; Ulzurrun and Zanuy, 2017). The load cell can be placed between the drop-weight and the tested specimen (Pham and Hao, 2016; Pham et al., 2018;

Wu et al., 2016) or embedded at the rear of an impact head (Fujikake et al., 2009; Yan et al., 2018; Zhou et al., 2019; Lee et al., 2018) as shown in Fig. 2. An investigation on the effects of load cell location and mass distribution of drop-weight on impact force has been reported in (Li et al., 2019b). When the load cell is placed between the drop-weight and the specimen, the mounted load cell changes the contact stiffness of the impact zone and leads to different profiles of impact force. Meanwhile, when the load cell is embedded at the rear of the impact head, the impact force measured by the load cell is lower than the actual contact force acting on the specimen due to the existence of the inertia resistance of the impactor head. The mass of impactor head determines the distinction between the measured impact force and the actual impact force. The heavier mass of impact head yields larger variations of impact forces. Therefore, the measured impact force is not necessary the actual impact force acting on the tested RC beam. Since the true dynamic response of a specimen is determined by the actual impact force on the RC beam, it is essential to distinguish the measured and actual impact forces to assess the load-carrying capacity of the RC beam and also for the accurate calibration of a numerical model. It is recommended that the impact force should be measured by the direct method which uses a load cell incorporated to the weight without an impactor head or with a light impactor head (to minimize its inertia resistance).

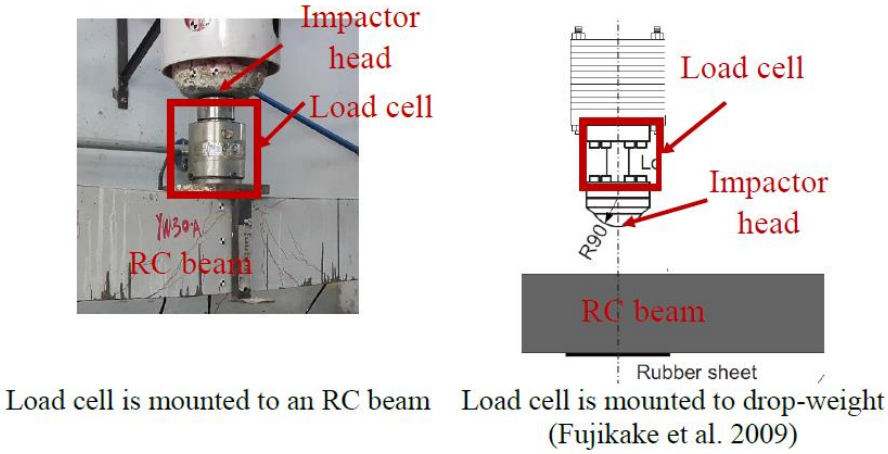

Load cell is mounted to an RC beam Load cell is mounted to drop-weight (Fujikake et al. 2009)

Fig. 2. Different locations of impact load cell and impactor head

In the previous impact tests (Li et al., 2018), the data acquisition system with the sampling rate of 50 kHz has been used to measure the impact force. It should be noted that the original signal of impact force should not be over-filtered as the impact force comprises the high-frequency contents. The peak value of the impact force can be underestimated if the signal is over-filtered. Remennikov et al. (2013) recommended using the low-pass fourth-order Butterworth filter in accordance with ISO 6487:2015 (1987) to process the measured signals. However, no clear justification was discussed. Meanwhile, for the strain gauge type of load cells, the impact force is measured from the strain distributed around the steel core of the load cell. The measurement accuracy of the impact force could be affected by the strain rate effect of the steel core itself during the impact event, which has not yet been systematically investigated. Soleimani and Banthia (2014) stated that a quasi-static calibration was deemed appropriate for the load cell since its modulus and ultimate strain do not considerably change under a high load rate. This statement has relied on the previous study by Fu et al. (1991) who concluded that the modulus of elasticity and ultimate strain of steel are almost constant while the yield stress and yield strain increase with the loading rate. It should be noted that various load cells are made of different high alloy steel materials, which shows strain rate sensitivity as reported in (Lee and Lam, 1996; Lichtenfeld et al., 2006). In these studies of the high-strength alloy steel material subjected to high strain rate, the dynamic true stress is sensitive to high rate loadings but the elastic modulus remains the same. In experimental testing, the actual strain of a load cell is measured and converted into force via static elastic modulus of the load cell. The measured strain has already been the dynamic strain and it is converted to the dynamic stress/force by using the same conversion factor. Therefore, the normal calibration factor for a load cell, associated with static loads, can be used to measure impact force.

As mentioned previously, the location of the load cell greatly affects the measured impact force and impact response due to the inertia resistance of the load cell and impactor head and contact stiffness. To quantify the effect of the position of the load cell, two different setups from the previous studies are discussed herein. When a load cell is mounted to an impactor so-called Case 1, the actual impact location occurs between the steel load cell and a concrete beam. On the other hand, if a load cell is mounted on top of a concrete beam, namely as Case 2, the impact event actually happens between a steel impactor and the steel load cell. For Case 1, the load cell measures the impact force behind the impactor head and thus is affected by inertia resistance of the impactor head. For Case 2, a portion of the kinetic energy transfers to accelerate the load cell first and then the beam. It means that the imparted energy in the beam is smaller than the initial kinetic impact energy. In the previous study, Pham and Hao (2017b) used a load cell weighing 20 kg mounted it on top of a concrete beam of 150x250x1900 mm^3 (~171 kg). It is also well-known that a "shear plug" likely to occur during impact tests (Pham and Hao, 2016; Saatci and Vecchio, 2009) as shown in Fig. 3. The inertia force of this shear plug plus the dynamic shear resistance of the beam primarily resist the peak impact force (Yi et al., 2016). If the shear cracks are assumed as approximately 45^o, the mass of the shear plug which primarily affects the peak impact force is 36 kg. In this case, the mass of the load cell is about 55% of the shear plug and thus significantly affects the kinetic energy transferring to the shear plug. In this case, the impact force transferred to the beam is very different when directly impacting to the beam without a load cell. On the other hand, these two impact scenarios have different contact interfaces since the actual impact occurs at the steel-concrete interface and the steel-steel interface for the first and second scenarios, respectively. This difference results in different impact forces due to changes in the contact stiffness. This difference in the test setup causes a variation in the impact force and thus impact response of concrete beams which may lead to misleading observations and conclusions. Therefore, it is

necessary to consider the influences of different setups in analysing the impact response and comparing results of different studies to ensure that a similar test setup is adopted.

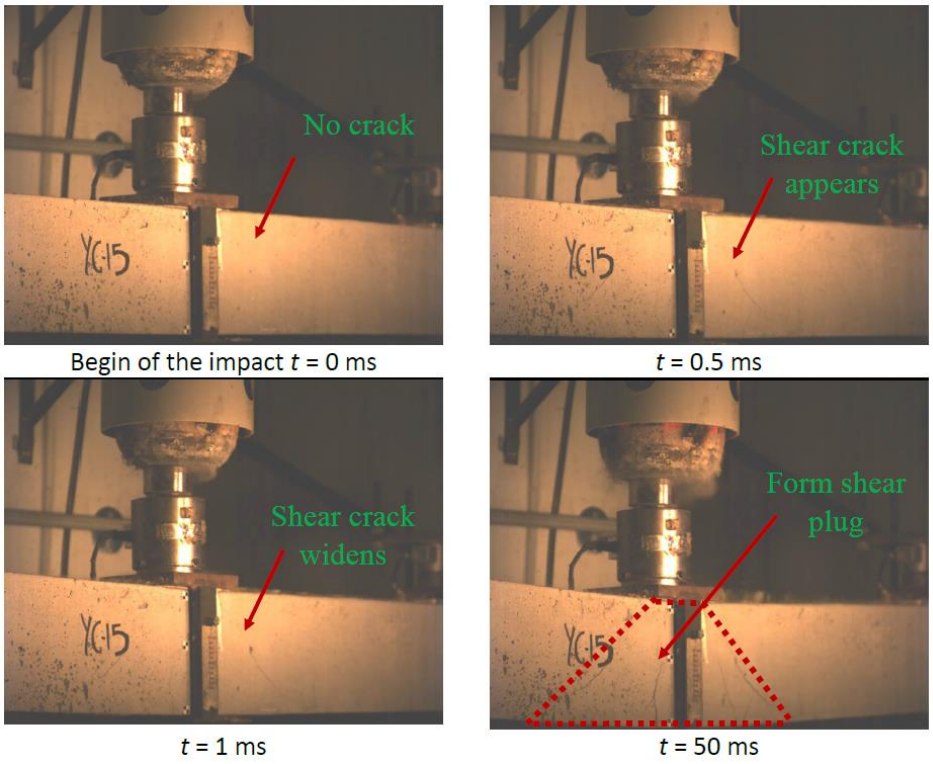

Fig. 3. Formation of shear plug under impact tests

An impact event happens in a very short period with an order of millisecond and thus is associated with very high-frequency signals. As mentioned previously, an appropriate data acquisition system should be fast enough to capture the true response of the structures otherwise peak values may be missed. The impact force duration is dependent on the time the impactor and specimen is in contact which is affected by both local and global stiffness of structures. For example, the first impact force duration of simply-supported RC beams, which had different dimensions and stiffness, was about 2 ms (Saatci and Vecchio, 2009; Kishi and Mikami, 2012), 5 ms (Pham and Hao, 2017b; Zhao et al., 2017a) or even 20 ms (Fujikake et al., 2009; Kishi et al., 2002a). In general, the first impact force duration of a "softer" RC beam is longer than that of a "stiffer" RC beam. Therefore, an appropriate data acquisition

system that is fast enough to capture the dynamic response of tested beams needs be properly selected based on the impact and beam conditions. The summary presented in Table 1 indicates that the sampling rate varying from 2.4 kHz to 250 kHz was used in the previous studies (Kishi and Mikami, 2012; Saatci and Vecchio, 2009; Silva et al., 2009; Tang and Saadatmanesh, 2005; Wang et al., 1996; Bhatti and Kishi, 2011; Zhan et al., 2015; Wu et al., 2015; Goldston et al., 2016; Soleimani and Banthia, 2014; Kishi et al., 2002a; Erki and Meier, 1999; Liu and Xiao, 2017; Tang and Saadatmanesh, 2003; Fujikake et al., 2009; Zhao et al., 2017a; Hughes and Mahmood, 1984; Bhatti et al., 2009; Banthia et al., 1987; Tachibana et al., 2010; Adhikary et al., 2013; Hughes and Beeby, 1982). Some early studies with quite low sampling rates (< 10 kHz) was reported more than a decade ago while recent studies used higher sampling rates (50-250 kHz). Specimens of these studies had different cross-sections and span lengths, and the responses were recorded with different sampling rates. It is difficult to make a direct comparison between these samples to suggest an appropriate sampling rates for this type of drop-weight tests. Previous studies have proven the numerical model can reasonably predict the impact responses of RC beams (Pham and Hao, 2017d; Pham and Hao, 2017c; Pham and Hao, 2018; Pham et al., 2018). Accordingly, the impact force time history from the numerical model is presented in the time and frequency domains as shown in Fig. 4. The highest frequency component of the signal is about 5 kHz. It is commonly recommended that the sampling rate should be at least two times the expected frequency. As a result, the minimum sampling rate of 10 kHz should be used for drop-weight tests on simply-supported RC beams. This recommendation means that using a data acquisition system with a sampling rate of less than 10 kHz is not sufficient for impact tests and peak impact forces could have been missed. In addition, to prevent information loss or test stiffer beams, it is recommended to sample at five to ten times the highest expected frequency rather than the minimum two times. Therefore, the sampling rate of about 50 kHz is appropriate which can provide a safety factor to guard against information loss. It is noted that this recommendation applies to

simply-supported RC beams which have similar dimension and stiffness to those in Table 1. It may require a higher sampling rate if stiffer beams are tested.

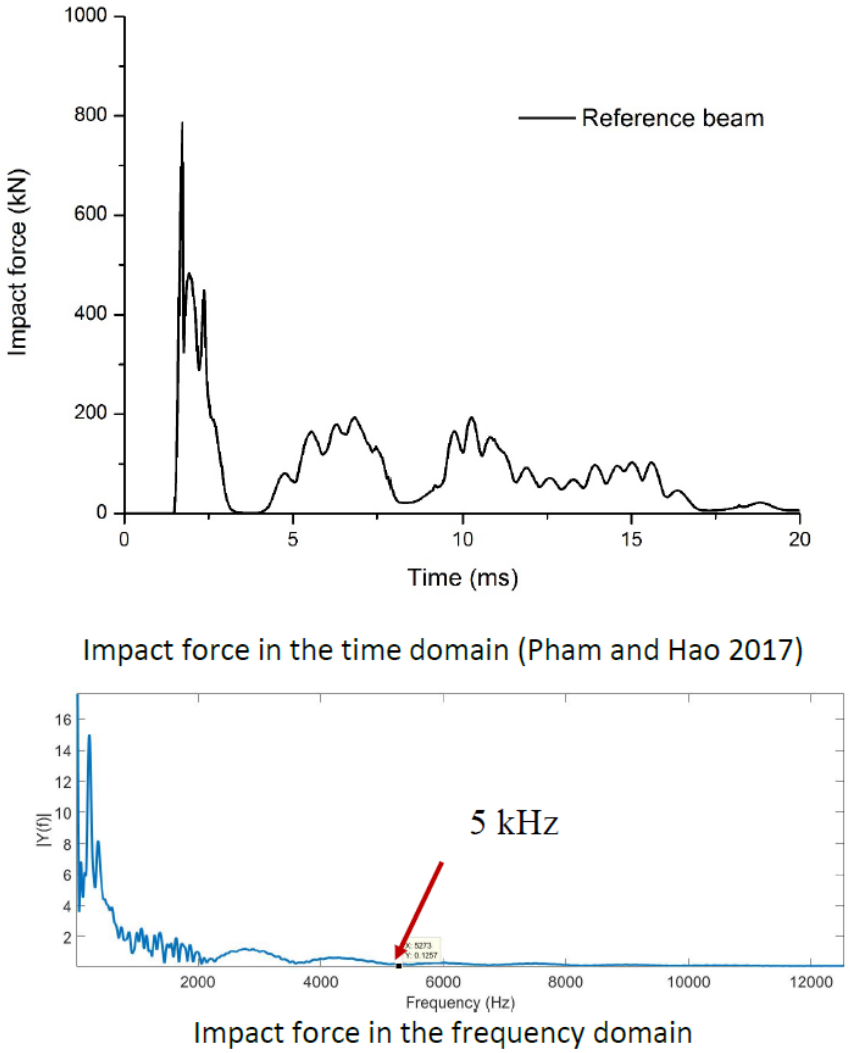

Fig. 4. Impact force in time and frequency domains

In addition, the geometry of the impactor head also plays an important role and may considerably affect the impact response of RC beams. In the previous impact tests, the impactor heads had various geometries including flat (Anil et al., 2016; Yan et al., 2018; Saatci and Vecchio, 2009; Yilmaz et al., 2014; Pham et al., 2018; Chen and May, 2009), wedge (Zhan et al., 2015), hemispherical (Chen and May, 2009; Fujikake et al., 2009; Adhikary et al., 2015; Zhao et al., 2017b) and curved surface with different curvature radius

(Tachibana et al., 2010; Kishi et al., 2002b; Kishi and Mikami, 2012) as shown in Fig. 5. The effects of various geometries of an impactor head on the impact behavior of RC beams have been investigated in the previous study (Li et al., 2019a). The variation in the drop-weight head leads to different contact stiffness which is based on the penalty method in LS-DYNA (Hallquist, 2006) and is given as $k = \frac{f_s K A^2}{V}$, where f_s is the scale factor for the contact stiffness and its default value is 1.0, K is the bulk modulus of contact materials, A and V are the contact area and the volume containing the contact elements, respectively. Different impactor heads lead to dissimilar contact areas, which affects the contact stiffness and therefore the impact force. The drop-weight with a flat head generates the highest impact force while the impact head has a very limited effect on the displacement response of RC beams with the same impact energy input (Li et al., 2019a). Various impact heads lead to different damage of RC beams, i.e. more severe damage is observed at the impact zone for the drop-weights with hemispherical and curved heads while a drop-weight with flat head causes more damage at the negative bending moment region. It is worth noting that the initial inclination angle (e.g. 1 or 2 degree) of a drop-weight is possible in the impact tests (Li et al., 2019a). The peak impact force is very sensitive to the change of the initial inclination angle of drop-weight with flat head. Fortunately, the effect of initial inclination angle on the impact force can be minimized by using the drop-weight with hemispherical and curved heads. Therefore, the drop-weight geometries should be considered in the impact rig design to obtain the accurate impact loading profile and dynamic behaviour of the beams. In reality, an impact event may occur between two objects not necessarily at flat surfaces but concentrates on a small contact area. To cope with impact events in practice, the use of a hemispherical or curved impactor head is recommended.

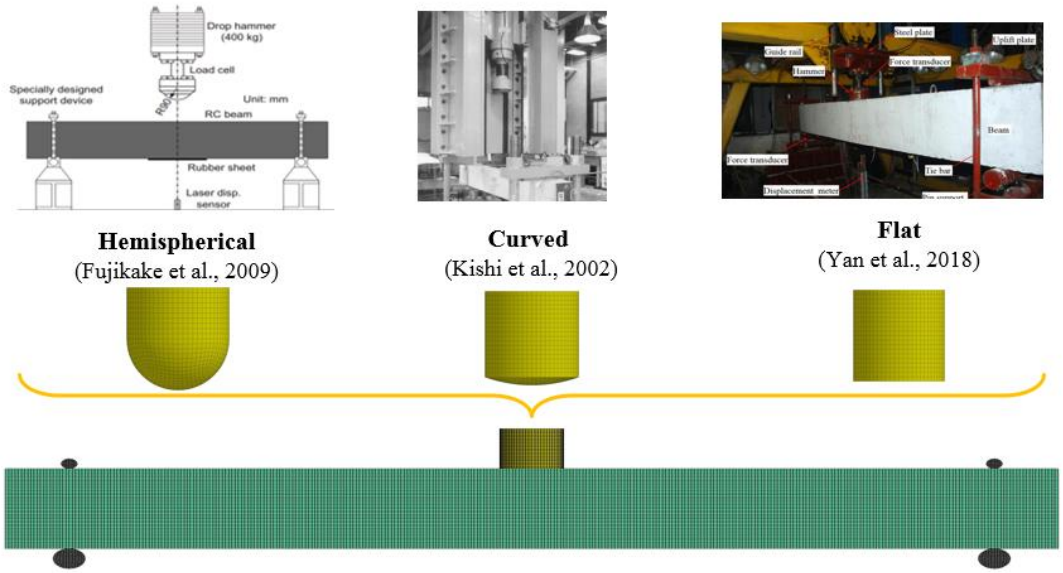

Fig. 5. Various geometries of impactor head

Beside the drop-weight directly impacting on the beams (Yan et al., 2018; Adhikary et al., 2015; Fujikake et al., 2009; Tachibana et al., 2010; Kishi et al., 2002b; Kishi and Mikami, 2012), steel plates (Saatci and Vecchio, 2009; Zhao et al., 2017b), rubber pads (Zhan et al., 2015), a combination of steel plate and rubber pad (Anil et al., 2016; Yilmaz et al., 2014) or plywood pads (Chen and May, 2009) have been used as interlayers between drop-weight and RC beams as shown in Fig. 6. By placing the rubber pads (Yilmaz et al., 2014; Anil et al., 2016; Zhan et al., 2015), possible oscillations and local failure can be mitigated. Using steel plates or plywood can provide even contact surface between drop-weight and RC beams and prevent severe localized damage at the impact zone (Saatci and Vecchio, 2009; Zhao et al., 2017b; Anil et al., 2016). It is worth noting that inserting various interlayers results in different contact stiffness of the impact zone. Li et al. (2019a) have numerically investigated the effect of different interlayers with steel and rubber material on the impact behavior of RC beams. It is found that higher impact force is generated by placing steel plates while a lower impact force is presented by placing rubber pads as compared to the direct impact on RC beams. RC beams might experience larger displacement response by placing a rubber pad as

interlayer, which is due to more impact energy transferred to the beam. In summary, the use of interlayers with different material and thickness presents different contact stiffness at the impact zone, which greatly affects the impact behaviour of RC beams. The interlayers should be considered in designing impact tests to achieve a desired impact force profile and reflect the actual impact conditions. As compared to the scenario without an interlayer, using an interlayer such as a steel plate has the advantage of generating well-distributed impact force throughout the width of beams and mitigating severe local concrete damage at the impact zone. To obtain higher peak impact force with a shorter duration for specific testing purposes, steel plates can be employed onto the beams owing to the stiffer impact zone as compared to the scenario of direct impact. Meanwhile, the rubber pads can be placed onto the beams to generate the impact load profile with lower peak force but longer duration. There is no universal interlayer fitting all scenarios, the interlayer should reflect the true contact stiffness which is being considered. It should be noted using rubber pads generates larger displacement response, which is due to higher impulse imposing onto the beams.

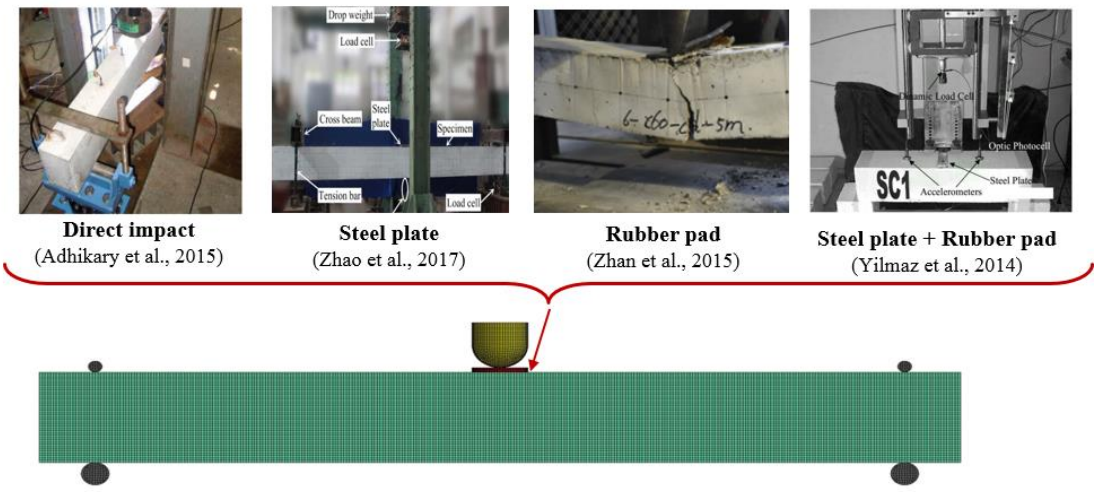

Fig. 6. Various types of interlayer

Reaction forces

Different from the static case, the reaction forces of RC beams under impact loading consist of positive and negative reaction forces. The reaction force in the upward direction is assumed positive reaction force which is similar to the case of static tests while the reaction force in the downward direction has a negative sign. The previous studies have reported that the negative reaction forces were recorded before their counterpart positive reaction forces (Pham and Hao, 2017b; Kishi and Mikami, 2012; Zhao et al., 2017a). In the meantime, the other studies on the drop-weight tests did not observe this phenomenon and only positive reaction forces were recorded (Kishi et al., 2002a; Pham and Hao, 2016; Fujikake et al., 2009; Saatci and Vecchio, 2009; Bhatti et al., 2009). This interesting phenomenon was also confirmed by a numerical investigation by Cotsovos (2010) who reported that a negative reaction appears prior to the positive reaction when a beam is loaded under a high loading rate. Pham and Hao (2017b) suggested an explanation based on the stress wave theory. When an impactor strikes a solid surface and induces stress waves that propagate in the solid. Among these stress waves, the surface Rayleigh wave accounts for 67% while Shear and P-wave are attributed to the remaining 26% and 7% of the impact energy, respectively (Rhazi et al., 2002). P-wave and shear wave propagate faster than Rayleigh wave and diminish faster because they possess relatively higher frequency contents. For drop-weight tests on beams, stress waves are also generated and propagate from the impact point towards the supports. As a result, P-wave reaches the support first, followed by the shear wave and then Rayleigh wave. P-wave propagates in the longitudinal direction while shear wave travels in the transverse direction, at which these two waves cause the beam to vibrate in the horizontal direction. It is obvious that horizontal vibrations of the beam do not induce vertical load and thus the arrival of P-wave and shear wave are not detected by the load cell placed in the vertical direction. On the contrary, Rayleigh wave induces the vertical vibration with elliptical wave path along the beam surface. As a result, the arrival of Rayleigh wave will be measured by the vertical load cell and results in negative reaction forces as reported by previous studies (Pham and Hao,

2017b; Kishi and Mikami, 2012; Zhao et al., 2017a). In general, this observation needs further investigation. It is not exactly clear yet when negative reaction forces should be expected and what causes this phenomenon. More investigation on this matter is deemed necessary.

To measure the negative reaction force (uplift force), the supports of RC beams need to be restrained in two directions and incorporate one or two load cells. There are two different setups for simply-supported beams including using (1) one load cell at the bottom of the beam and pre-stressed bolts (Kishi and Mikami, 2012; Fujikake et al., 2009) or (2) a load cell at each side of the beam to measure the positive and negative reaction forces (Pham and Hao, 2016; Pham and Hao, 2017b; Pham et al., 2020) as shown in Fig. 1. In the first method, steel bolts need to be pre-stressed at a greater level than the negative reaction force. It means that the bottom compression-only load cell is loaded with a load level greater than the negative reaction force. As a result, when the negative reaction force appears, it reverses the reading on the load cell and thus can measure both negative and positive reaction forces. When using this method, the top and bottom surfaces of the beams are lumped as one point at the load cell. Therefore, stress waves on the top surface of the beam are not accurately monitored. On the other hand, both the negative and positive reaction forces and the surface stress waves can be measured by using two load cells as mentioned in method 2. Therefore, the use of two load cells is suggested to succefully capture the negative reaction force caused by either global beam response or surface stress wave.

Shear dominance in impact tests

There is another interesting phenomenon of the shear dominance in impact tests, which is worth mentioning herein. The previous studies have shown that RC beams more likely to fail by shear when subjecting to high-velocity impact (Saatci and Vecchio, 2009; Pham and Hao, 2017b; Pham and Hao, 2017d; Pham and Hao, 2017c; Pham and Hao, 2018; Pham et al.,

2018). Pham and Hao (2017b) carried out an experimental investigation on RC beams which had the shear resistance 3.42-4.08 times higher than their flexural strength. The failure of these beams under static loads is primarily governed by vertical flexural cracks as shown in Fig. 7. However, the identical beams failed by a combination of shear-flexural cracks. The crack patterns of these beams have shifted from vertical cracks in static tests to both inclined and vertical cracks under impact loads. The shear dominance in impact tests was also reported in the previous studies (Saatci and Vecchio, 2009) and explained by (Pham and Hao, 2017b). When a drop-weight strikes a beam and accelerates it, the beam maintains its equilibrium at any time instant associated with impact force, reaction forces, and inertial forces as shown in Fig. 8. From the experimental results and numerical investigation, Pham and Hao (2017d) indicated that the beam is balanced primarily by the inertia resistance of the beam portion close to the impact point and the shear resistance at the very early stage after the impact. The findings are supported by the experimental results of previous studies that only a portion of the beam is accelerated right after the impact while the rest of the beam remains stationary. It also means that after a very short time duration after the impact, the reaction forces of the beam is still zero.

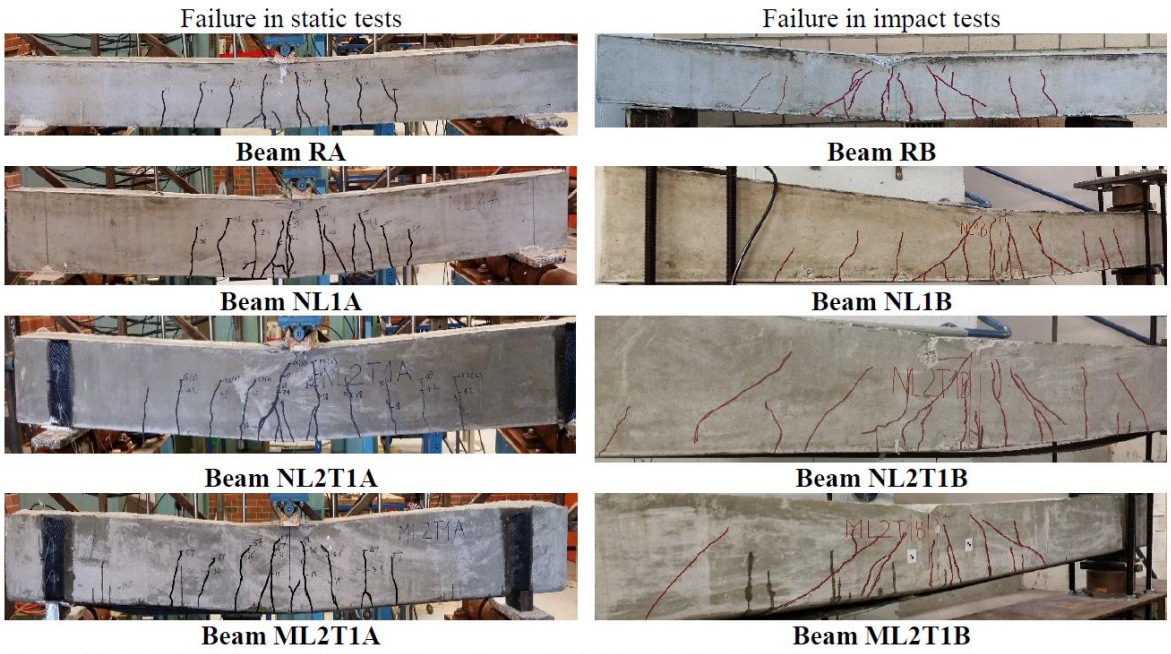

Identical beams failed differently under static and impact tests (Pham and Hao 2017)

Fig. 7. Shear dominance phenomenon

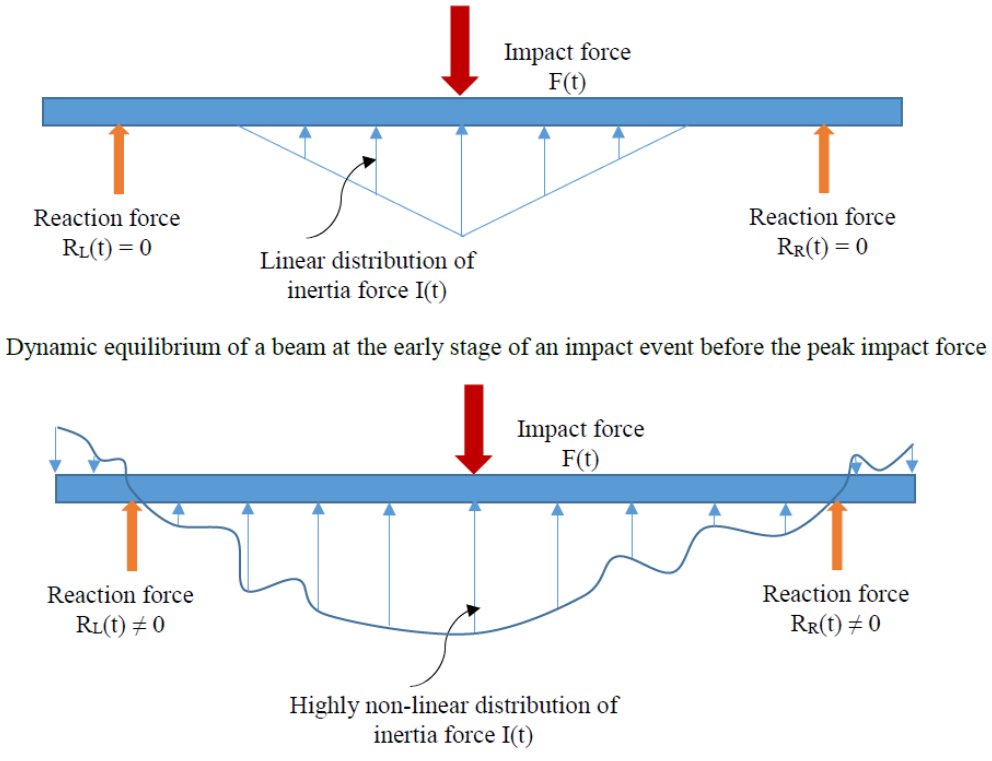

Fig. 8. Dynamic equilibrium under impact loads

From the above review and analysis, it can be concluded that when an impactor strikes a beam, the local shear response will occur first following by the global response. If the maximum impact force is smaller than the dynamic shear resistance, the beam may fail in a flexural manner. It is worth mentioning that the dynamic shear resistance of a beam consists of the actual dynamic resistance of materials and inertia resistance of the shear plug as shown in Fig. 9 (Do et al., 2019a). It has been proven in the previous study by Do et al. (2019a) that the flexural response only occurs if the dynamic shear resistance of a structure is greater than the peak impact force. Otherwise, concrete structures show punching shear failure at the impact area. The dynamic punching shear resistance, V_D, can be estimated as follows (Do et al., 2019a):

$$V_D = V_C + V_s = k_T f_t bh = 6.5 \frac{f_c}{10} bh \quad (1)$$

where V_C and V_S are respectively the contribution of concrete and steel reinforcements to the dynamic shear resistance, k_T is the dimensionless coefficient which considers the effect of dynamic increase factor (DIF) and inertia force in the shear plug area, which is taken as 6.5; f_c and f_t are the compressive and tensile strengths of concrete, respectively; and b and h are the width and height of cross-section, respectively. The dimensionless coefficient of 6.5 in Eq. 1 for the dynamic shear resistance of a concrete structure accounts for both the dynamic increase factor of material strength and the inertia resistance of the shear plug that contribute to the shear capacity. The inertia force of the shear plug depends on its mass and acceleration. Intensive numerical simulations were carried out together with regression analysis to obtain the coefficient. This coefficient was discussed in detail and suggested in the previous study (Do et al., 2019a). It is not the conventional DIF of material strength, but a DIF of structural shear capacity. It is higher than the DIF of material strength because of the contribution of inertial resistance to impact resistance.

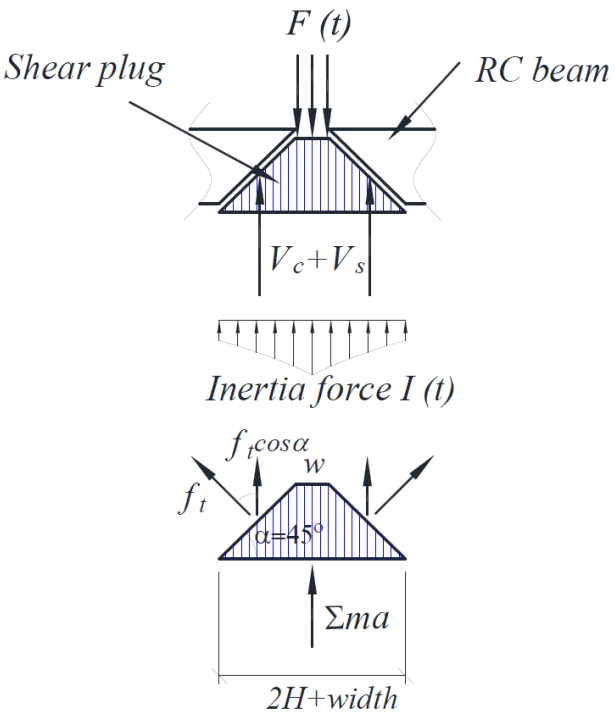

Fig. 9. Dynamic shear model

Results from the previous study have also been collected to verify the dynamic shear resistance of RC beams as shown in Table 2. It can be seen that RC beams which showed punching shear failure had the peak impact force very close to its dynamic shear resistance. Therefore, this formula can be adopted to predict whether punching shear failure (shear plug) may occur in RC beams.

Analytical investigations

The impact responses of steel beams were studied well before concrete beams since it was found the standard static methods of analysis with dynamic magnification factors showed inadequate prediction on the dynamic response (Jones, 2011). For example, early static and dynamic tests on buses exhibited distinguished behaviour and failures of the structure under static vs dynamic loadings (Liu and Jones, 1987). After reviewing these results, Jones (2011) concluded that an analysis of a bus subjected to static longitudinal loads is of little relevance to its design against dynamic loads. Therefore, actual dynamic tests and analyses are required

to provide a better understanding of the impact problem. Analytical solutions for perfectly plastic beams were presented in the previous study by Jones (2011) in which material elasticity was neglected in the dynamic case owing to large deformation problems and only a small amount of energy absorbed in a wholly elastic manner. The analytical solution is applicable for a simply-supported beam subjected to a uniformly distributed pressure pulse or a fully-clamped beam struck by a flying mass at the mid-span or tip. The complete solutions and discussions for such problems were presented in detail in previous studies (Jones, 2011; Biggs, 1964; Johnson, 1972; Stronge and Yu, 1993). Some assumptions, which were used in these solutions, require careful justification. For example, the linear distribution of the velocity and acceleration along the beam is assumed to derive the analytical solutions. This assumption is not necessarily correct for the entire impact duration of a concrete beam, which will be discussed later. The influence of transverse shear and rotatory inertia were also discussed in (Jones, 2011) but the shear strain was assumed as zero which is not appropriate for concrete beams since they are very sensitive to shear strain. When solving for the travel time of a plastic hinge from the mid-span (the impacted position) to the supports, the assumption that a plastic hinge forms at the impact points at t=0 is made (Jones, 2011) or the impact force is equal to the static collapse force at t=0 (Stronge and Yu, 1993). It is noted that the static collapse force is defined as the applied load causing the plastic bending moment. In practice, however, a plastic hinge is developed only when the bending moment at that section exceeds the plastic bending moment. Consequently, the bending moment at the mid-span requires a short duration to reach the plastic bending moment. As a result, a plastic hinge at the mid-span is formed only after a certain duration instead of instantaneously upon impacting. These assumptions (Jones, 2011; Stronge and Yu, 1993) are simplifications of the problem for the plastic hinge propagation analysis. Additionally, a solution was also presented in the previous study by Johnson (1972), in which the inertia force is assumed to distribute uniformly along the beam. In general, this type of model can be used to estimate the dynamic

load-carrying capacity of a steel beam but its application for concrete beams requires some modifications, which will be discussed in this study.

Spring-mass model

The dynamic responses of RC beams to impact force and displacement under impact loads can be analytically modeled by using either single-degree or multiple-degree of freedom spring-mass models (Wu and Yu, 2001; Wang et al., 1996; Suaris and Shah, 1981; Fujikake et al., 2009; Bischoff et al., 1990; Anderson, 2005) (see Fig. 10). These studies assumed the beam as a lumped mass supported by a spring. One of the pioneer studies using a single degree of freedom (SDOF) model for a beam under impact loads was reported by Lee (1940) in 1940. At that time, Lee (1940) assumed only elastic impact in his solution. Later studies proposed two-degree-of-freedom (TDOF) models to investigate the impact response of a beam (Fujikake et al., 2009; Suaris and Shah, 1981; Abrate, 2005; Bischoff et al., 1990). Details of these models are not presented here for brevity. Only the key parameters of these models including the stiffness, equivalent mass, and effective length will be discussed.

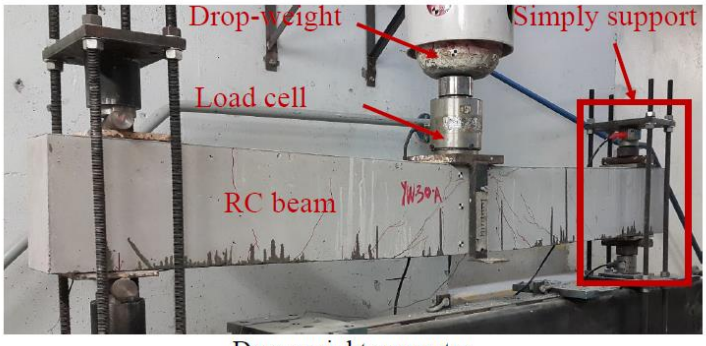

Drop-weight apparatus

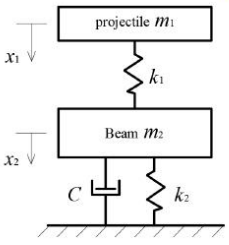

2DOF model

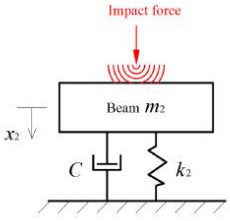

SDOF model

Fig. 10. Spring-mass model

There are various methods to estimate the equivalent spring stiffness from beam properties in the spring-mass models according to its structural effects, i.e. flexural, shear, or indentation stiffness (Dragos and Wu, 2014; Low and Hao, 2002; Krauthammer et al., 1986; Ross and Krawinkler, 1985; Pham and Hao, 2018). Using a spring-mass model for an impact problem might yield reasonable predictions if the global response mode is dominant (Hao, 2015; Pham and Hao, 2017d; Pham and Hao, 2017c). In addition, a spring-mass model separately considers the shear and flexural responses. This common approach is often adopted since these two responses normally do not happen simultaneously. A beam exhibits the flexural response mode only if it can withstand the maximum shear force (Low and Hao, 2002). Krauthammer et al. (1993) separately model the flexural and direct shear responses in SDOF analyses. Meanwhile, loosely coupled SDOF systems, which simultaneously take account of both the flexural and shear failures, were proposed in other studies (Xu et al., 2014; Low and Hao, 2002). The previous studies have shown that modelling the structural responses using the assumption of global flexural and/or shear responses does not always yield reasonable predictions because the responses might be governed by local responses upon impact, i.e., impact only activates a limited portion of the beam to resist the high-speed impact loads and induces significant damage to the local area of the beam before the occurrence of the global beam responses. Therefore, the estimation of the equivalent beam stiffness and mass for predicting the local and global responses requires careful justifications. The equivalent local stiffness and mass should be estimated when modeling the local responses within a very short duration of the impact force phase and then change to the equivalent global stiffness and mass for simulating the impact response of RC beams during the free-vibration phase.

Similarly, there are a few approaches to determine the equivalent mass in a spring-mass model. It is noted that the equivalent mass of a spring-mass model is different from the

physical mass of the real beam. Wu and Yu (2001) estimated the equivalent mass for a simply-supported beam by equating the fundamental frequency of a beam to that of the spring-mass model. As a result, the equivalent mass of a beam is equal to $48/\pi^4$=0.493 of the real mass. Meanwhile, Fujikake et al. (2009) proposed a TDOF model with the equivalent mass equal to 17/35 (0.486) of the physical mass. Biggs (1964) equated the displacement of a real structure and the equivalent spring-mass model. The ratio between the equivalent mass to the real mass of a fixed-beam varies from 0.33 for the plastic response case to 0.5 for the elastic-plastic response case (Biggs, 1964). The equivalent mass of a model corresponding to a vibration mode is computed based on the real mass and the assumed shape function (Hao, 2015; Do et al., 2019b). Yi et al. (2016) coupled the equivalent mass with the actual response of a beam, i.e. the equivalent mass is equal to the mass of the shear plug at the local response phase while it is computed based on the entire beam when the global response comes into effect. All the above procedures of estimating the equivalent mass are based on the global response assumptions. As discussed above, the response of a beam upon impacting is dominated by local response and this localized response may induce significant damage to the RC beam. Therefore, for reliable prediction of local beam responses, equivalent local mass needs be estimated, similar as to estimating the equivalent local stiffness. An analytical spring-mass model for RC beams subjected to impact loads should be derived by taking into consideration both the local and global responses. By considering both local and global response, an analytical method proposed by Li et al. (2021) provides close prediction to the experimental testing. The analytical model adopted the penalty contact algorithm for the local stiffness of a flat-head projectile (LS-Dyna, 2012) while the Hertz contact model is utilized for curved-head projectiles (Machado et al., 2012).

Besides, the effective length also plays an important role in a spring-mass model. Many previous studies assumed the effective span between two supports for their models (Wu and

Yu, 2001; Fujikake et al., 2009; Pham and Hao, 2018). This approach can be used when considering the global response of a beam. On the other hand, a much shorter effective length should be used during the local response phase, which usually coincides with the impact force phase because not the entire beam is activated to resist impact load in the initial stage (Pham and Hao, 2017c; Pham and Hao, 2018; Yi et al., 2016). The effective length during the local response phase is estimated as the span between two inflection points (Yi et al., 2016) or two plastic hinges (Pham and Hao, 2017d; Cotsovos, 2010) but not the actual span of the beam. Therefore, when modeling the impact response during the impact force phase, the effective span should be used rather than the total span between two supports. As can be seen that the three important parameters, including the equivalent stiffness, equivalent mass, and effective span, in a spring-mass model can be estimated in various ways. Therefore, to achieve reliable predictions, the estimation of these three parameters requires due care with good understanding of the corresponding mechanisms of a RC beam subjected to impact loads.

Energy-balance model

In addition, the energy-balance method was also utilized to examine the impact force in an impact event (Abrate, 2001; Hazizan and Cantwell, 2003; Foo et al., 2011; Zhou and Stronge, 2006). The initial kinetic energy of an impactor causes deformation of a beam and it is commonly assumed that the impact velocity becomes zero when the beam reaches its maximum deflection. All the kinetic energy is thus transferred to the beam if the energy loss is neglected. Based on the conservation law of the kinetic energy and total energy, the energy-balance equation can be formed in which the energy composition includes the bending deformation, shear deformation, membrane component, and indentation effect. Various assumptions were made to neglect some energy compositions for particular scenarios, for example, Hazizan and Cantwell (2003) neglected the membrane effect while Abrate (2005) ignored the indentation effect. This type of model relied on assumptions that are difficult to

achieve in reality and it can only estimate the peak impact force which is insufficient for a detail analysis of an impact problem. Therefore, although the energy-balance models can serve as an alternative solution but they are less popular than the others.

Assumptions and limitations

To analyse the impact response of RC beams, previous studies assumed the linear distribution of the inertia force along a beam under impact loads (Banthia et al., 1987; Goldston et al., 2016; Saatci and Vecchio, 2009). The inertia force is usually computed from measured acceleration along a beam. It is worth mentioning that the acceleration signals monitored by accelerometers fluctuate significantly. The linear distribution assumption has been used for a long time without careful justification. Pham and Hao (2017d) analysed the acceleration signals measured by Saatci and Vecchio (2009) and found that the acceleration only linearly distributes along the beam in a very early stage of an impact event up to the maximum impact force then it varies significantly afterward. This observation was also confirmed by comparing with the numerical simulation (Pham and Hao, 2017d). Therefore, it is recommended that the use of the linear distribution of inertia force along the beam is applicable up to the maximum impact force only.

The damping effect is usually adopted in spring-mass models but its application has not been carefully justified. Many previous studies ignored the damping effect due to its limited influence within a short period during an impact event (Pham and Hao, 2017d; Pham and Hao, 2017c; Abrate, 2001; Olsson, 2000; Bischoff et al., 1990; Saatci and Vecchio, 2009). Typical damping ratios of RC structures range from 2% to 5% under conventional working conditions, but when the structures exhibit large deformation (i.e. in many impact problems), the structural damping ratio might exceed 10% (Krauthammer et al., 1986). This justification has not distinguished clearly two different phases of the beam response under impact loads,

namely the impact force phase and free vibration phase (Pham and Hao, 2017d; Pham and Hao, 2017c; Pham and Hao, 2018; Pham et al., 2018). The usual impact force phase vanishes in a very short period (1-5 ms) while the duration of the free vibration phase lasts much longer up to 100 ms, depending on structures and contact condition. As a result, ignoring the damping effect in the force phase is acceptable but the damping effect should be considered in the free vibration phase. Pham and Hao (2018) proposed a spring-mass model to predict the impact response of RC beams in which the damping ratio of an RC beam during the free vibration phase was assumed as approximately 3.5% while the damping effect during the force phase was ignored. The proposed model yielded quite close predictions to the experimental data. This assumption was also adapted by other studies that set the damping ratio as zero during the force phase and 5% during the free vibration phase (Yi et al., 2016; Fujikake et al., 2009). In general, the damping effect of these two phases should be different. The damping ratio during the force phase is not necessarily set to zero but its effect on structural responses is minimum, and the damping ratio should be different from that of the free vibration phase.

Numerical simulation

Although experimental investigations on the impact response of RC beams subjected to impact loads provide useful data and observation in the literature, these tests are expensive and time-consuming. Some information is very difficult or almost impossible to experimentally measure, i.e. stress state of concrete at the impact point, resulting bending moment and shear force at a section, and so on. Accordingly, numerical modelling can provide more detail information and also can be utilized to carry out intensive parametric studies. To build a numerical model for an impact problem, many information and knowledge are required, such as contact mechanism, constitute material models, failure criteria, dynamic

increase factor (DIF), erosion criteria, and etc. These mechanisms, models, and criteria will be reviewed and discussed in this section.

Contact mechanism

The contact mechanism greatly affects the impact response of an RC beam in which the contact stiffness between an impactor and an RC beam plays an essential role. Even though there have been many studies on the contact mechanism and impact force prediction (Flores and Ambrósio, 2010; Shivaswamy and Lankarani, 1997; Flores et al., 2010; Alves et al., 2015; Machado et al., 2012; Dogan et al., 2012), the Hertz contact theory still serves as the base for most of the available contact models (Machado et al., 2012). These contact models can be classified into two types including contact force-based and geometric constraints based methods (Alves et al., 2015). Among these two methods, the contact force-based method is also known as the penalty approaches which has been used commonly in many numerical studies (Pham and Hao, 2017d; Pham and Hao, 2017c; Pham and Hao, 2018; Pham et al., 2018). Meanwhile, the geometric constraints based methods assume two rigid bodies contact and thus the relative indentation is zero. As a result, this contact mechanism does not reflect the actual response of an impactor-concrete beam and is not discussed in this review. On the other hand, the contact force-based method estimates the impact force based on a relative indentation of two contacting objects and the indentation determination obviously governs the contact force prediction. In this contact mechanism, the contact force is a function of the contact stiffness, the relative indentation and the indentation velocity. It is noted that the contact stiffness is represented by an artificial stiff spring between two contacting bodies. Even though the penalty approach has been used excessively and proven as a reliable method to simulate the impact problems between an impactor and an RC beam (Pham and Hao, 2017d; Pham and Hao, 2017c; Pham and Hao, 2018; Pham et al., 2018; Kishi et al., 2011; Jiang and Chorzepa, 2015; Villavicencio and Guedes Soares, 2011), this approach may cause

high-frequency dynamics in structures due to the interaction between a stiff spring and contacting surfaces (Shivaswamy and Lankarani, 1997). When using the penalty approach, a highly accurate estimation of the contact stiffness is required to achieve a reasonable prediction. If the high-frequency dynamics phenomenon occurs, the integration algorithm in the numerical analyses requires very small steps and thus makes the computational cost very expensive (Flores and Ambrósio, 2010). The determination of the contact stiffness is not a straightforward task and it requires intensive experiences on modelling and a good understanding of the contact mechanism. In addition, the contact stiffness was also found to be very sensitive to not only the relative indentation, material properties, kinematics of the contacting bodies, and surface geometries but also the actual contact surface condition as explained in the previous study (Pham et al., 2018).

Pham et al. (2018) experimentally tested two identical RC beams which had a similar design and material properties but different conditions of the contact surface. The steel load adaptor was placed directly on the first beam while a thin layer of plaster was used to ensure a good contact condition between the load adaptor and the second beam. The impact performance of these two beams was very different in terms of the impact force time history, crack patterns, bending moments and shear forces, and failure modes. The difference in the actual contact surface condition and thus contact stiffness can be modelled by using the AUTOMATIC SURFACE TO SURFACE (penalty method) in the finite element method i.e. LS-DYNA (LS-Dyna, 2012). To manipulate the contact stiffness in a numerical simulation, a scale factor is utilized and it has become a challenge in simulating a contact problem. The penalty factor plays as an essence of the penalty contact algorithms and it governs the reliability of the simulation (Mongeau and Sartenaer, 1995; Rubinov et al., 2002; Nour - Omid and Wriggers, 1987; Bednarek and Kowalczyk, 2013; Izi et al., 2013). Determination of the scale factor of the penalty method is difficult and can be very different for various impact problems, for

example, objects with similar stiffness (steel vs steel or concrete vs concrete), intermediate difference in stiffness (steel impactor vs concrete beam or hard impactor vs composite structures), and substantially different stiffness (ship vs water) (Wang and Guedes Soares, 2014; Dogan et al., 2012; Pham et al., 2018; Pham and Hao, 2018; Pham and Hao, 2017c; Pham and Hao, 2017d; Jiang and Chorzepa, 2015; Villavicencio and Guedes Soares, 2011; Kishi et al., 2011).

The commercial software LS-DYNA provides many contact algorithms to model impact problems, i.e. kinematic constraint, penalty, and distributed parameter methods (LS-Dyna, 2012). Dogan et al. (2012) discussed the pros and cons of these three methods, in which the penalty method (CONTACT_AUTOMATIC_SURFACE_TO_SURFACE) has gained popularity and yielded reliable predictions (Dogan et al., 2012). The penalty method is divided into subclasses including standard penalty formulation, soft constraint penalty formulation, and segment-based penalty formulation. The constraint penalty formulation can be used to model contact between bodies with substantially different material properties, such as steel vs foam. The stiffness determination and the corresponding update during the simulation using the constraint penalty formulation is different from that of the standard penalty formulation. Meanwhile, the segment-based penalty formulation is a powerful contact algorithm in which a slave segment-master segment approach is used instead of a traditional slave node-master segment approach. These various formulations are designed for different impact problems. For example, the segment-based penalty formulation was proven reliable when modelling airbag self-contact during inflation and complex contact conditions (LS-Dyna, 2012).

Determination of the contact stiffness remains a primary challenge for the use of the penalty method. The contact stiffness, k, based on the explicit penalty contact algorithm in LS-Dyna with $SOFT = 0$ is computed as follows:

$$k = f_s \frac{KA^2}{V} \quad for\ solid\ elements \tag{2}$$

$$k = f_s \frac{KA}{Max\ diagonal} \quad for\ shell\ elements \tag{3}$$

where K is the bulk modulus, A is the area of the contact region, V is the volume of the contact elements, and f_s is a scale factor which is a combination of the penalty scale factor (*SLSFAC*) and the scale factor (*SFS/SFM*) for slave and master penalty stiffness, respectively. The use of scale factor requires due care to ensure reliable numerical results (Wang and Guedes Soares, 2014; Dogan et al., 2012). This scale factor can be significantly varied to reflect the actual contact condition as discussed in the previous study (Pham et al., 2018). The contact stiffness is governed by the respective material properties of the contact objects and the contact surface. When two dissimilar materials are involved in an impact event, the contact stiffness is estimated based on the stiffness of the softer material. This estimation does not always generate close predictions owing to "too small" stiffness. Once this issue happens, the scale factor is usually utilized to manually modify the contact stiffness to generate reasonable predictions. Pham et al. (2018) recommended that the scale factors SFS/SFM should be carefully modified to reflect the actual contact surface condition, i.e. contact stiffness, particularly a proper calibration against experimental data is essential. The minor difference at the contact surface condition of the two beams in the study by Pham et al. (2018) requires significant modifications of the scale factors, for example, the values of 0.02/0.1 and 0.5/0.5 were used for the scale factors SFS/SFM of Beams 1 and 2, respectively. More discussion and recommendation on how to choose the scale factors SFS/SFM can be found in the previous study (Pham et al., 2018). Based on the previous study (Pham et al., 2018), it is recommended that the scale factors in a numerical model require a careful calibration with experimental testing data to verify the reliability of the contact modelling.

Material models and DIF

The commonly used concrete material models in hydrocode include HJC model (Holmquist and Johnson) (1994), KCC model (Karagozian and Case) (Malvar et al., 1997), RHT model (Riedel-Hiermaier-Thoma) (Riedel et al., 1999), CSC model (Continuous Surface Cap), etc. The concrete constitutive material models cover the aspects of strength criterion, equation of state (EOS), plastic flow and damage, and strain rate effect, which have been reviewed in previous studies (Hao et al., 2016; Brannon and Leelavanichkul, 2009; Cui et al., 2017). Four concrete constitutive models are widely used by researchers and engineers in simulating structural response to dynamic loads, namely KCC model (MAT072R3), HJC model (MAT111), RHT model (MAT272) and CSC model (MAT159) in LS-DYNA. KCC, HJC, and RHT models are developed based on the plasticity theory and damage theory. CSC model is developed based on the visco-plasticity and damage theory for roadside safety analysis. KCC model (MAT072R3) can well capture the concrete behaviours such as post-peak softening, confinement effect and strain rate effect, which makes it suitable for the analysis under static, impact and blast loads. HJC model (MAT111) considers the material as linear elastic before reaching the prescribed failure criterion. RHT model (MAT272) is developed as an improvement based on the HJC model (MAT111) by adding several new features. CSC model (MAT159) can determine the parameters based on the unconfined compression strength and the aggregate size (LSTC, 2007). KCC, RHT and CSC models are easy to use by assigning the unconfined compressive strength and density of concrete, and then other parameters can be automatically generated through the built-in algorithm of the model. For the HJC model, the key parameters are determined based on experimental data. Given the same unconfined compressive strength, RHT and HJC models show the compressive stress-strain curves with the perfect plastic flow after reaching softening point while CSC and KCC models show no perfect plastic flow region. CSC model shows a longer softening stage than KCC model, indicating more ductility. For the tensile stress, KCC model shows the most brittle behavior while RHT model exhibits the higher post-crack strength and largest

deformation capacity (Cui et al., 2017). The response of concrete structures under blast and impact loads by using four models have been compared and reported in (Cui et al., 2017). KCC, RHT and CSC models can give reasonably good predictions on structural response subjected to blast loads while HJC model greatly under predicts structural response. In ABAQUS, there are three main concrete constitutive models including smeared cracking concrete model, cracking model for concrete and concrete damaged plasticity models (Chaudhari and Chakrabarti, 2012). Among them, the concrete damaged plasticity model as a continuum, plasticity-based, and strain rate sensitive damage model is defined with two main failure mechanisms of tensile cracking and compressive crushing and it has been successfully and popularly used in the dynamic analysis of RC structures against impact or blast loads (Li et al., 2010).

Meanwhile, the dynamic increase factor (DIF), i.e., the ratio of dynamic strength to static strength is used to define the enhancement of concrete strength under high strain rate. Based on the experimental data, various empirical DIF models have been proposed, such as HJC model, RHT model, fib code, CEB code, and Hao's improved model (Hao and Hao, 2011). It is worth noting that Hao's improved model presents the true dynamic increase factors (DIFs) for compressive (Hao and Hao, 2011) and tensile (Hao et al., 2012) strengths of normal concrete by removing the structural effects such as lateral inertial confinement and end friction confinement from experimental data (Hao et al., 2013). Therefore, Hao's improved model is recommended for the strength DIF of normal concrete.

The commercial software LS-DYNA and/or ABAQUS/Explicit can be used for numerical simulation of RC structures subjected to intensive dynamic loads. LS-DYNA with more abundant concrete material models has been intensively used for RC structures under impact/blast loads (Wongmatar et al., 2018; Li and Hao, 2014; Pham and Hao, 2018). KCC model (MAT072R3) with the input of unconfined compressive strength has been popularly

used for the concrete material and its accuracy has been verified. The steel longitudinal rebars and stirrups of RC beams are usually simulated by using material model *MAT PIECEWISE LINEAR PLASTICITY (MAT024) with the DIF relationship proposed by Malvar (1998) and erosion criterion. The rebars are usually embedded into concrete by using the keyword *CONSTRAINED BEAM IN SOLID.

Other issues

When subjected to dynamic loadings, a concrete element might experience large deformation, which can lead to singular Jacobi matrices, mesh tangling and computational overflow. To address this issue, erosion algorithm e.g. *MAT ADD EROSION in LS-DYNA is used to delete the concrete elements that the predefined failure criterion such as the maximum principal strain is reached. To simulate the concrete failure, the erosion criteria can be defined based on strain and stress limits. The strain-based erosion criteria can be defined based on effective strain, maximum principal strain, maximum shear strain, incremental geometric strain, and effective plastic strain. The stress-based erosion criteria include pressure, principal stress, and effective stress, etc. There is no best erosion criterion but more appropriate erosion criterion to reproduce the failure mode. The same phenomena can be simulated by various erosion criteria. The erosion criterion based on strain can better simulate the spalling phenomenon. In addition, two erosion criteria can be defined simultaneously and the erosion can be activated when either criterion is first reached. It is worth noting that the simulation of damage pattern depends on both mesh size and erosion limit. Meanwhile, the erosion limit based on strain is well dependent on the mesh size. For instance, a concrete slab with a dimension of 1.2 m by 1.2 m and a thickness of 0.32 m was subjected to contact explosion and the concrete slab damaged as reported in the previous study by Rabczuk and Eibl (2006). Subsequently, Luccioni et al. (2013a) conducted numerical simulations of this concrete slab and reported that the effective strain as erosion criterion was determined as 0.001 and 0.0002

for the mesh size of 2 mm and 10 mm, respectively to obtain similar failure modes as the experimental results (Rabczuk and Eibl, 2006). Therefore, it is suggested that the correlation between mesh size and erosion limit requires careful justifications in numerical simulations.

To compromise the computational cost and accuracy, the fine mesh is usually defined in the local contact area and coarser mesh is used for the remaining zones. Luccioni et al. (2013a) gave a summary of the erosion limit values for concrete material. It is worth noting that the erosion algorithm is a numerical manipulation and has less physical meaning. The mass conservation can be breached by excessive deletion of elements. Therefore, to maintain mass conservation, the mass of deleted elements is suggested to be retained in the model.

In addition, the excessive distortion of elements could cause negative volumes, which could terminate the simulation. To prevent this, the elements with excessive distortion of elements should be deleted or a single integration point should be employed in numerical code. Meanwhile, without hourglass control, the elements could experience zero energy deformation modes, which could lead to inaccurate outcomes (LSTC, 2007). Therefore, the hourglass energy should be kept below 10% of internal energy to ensure that the contribution from spurious energy is low enough. The contact keyword *CONTACT AUTOMATIC SURFACE TO SURFACE in LS-DYNA based on penalty method is used to define the contacts between drop-weight and RC beams. The scale factors (SFS/SFM) for contact stiffness can be determined by calibrating the impact force, as detailed in (Pham et al., 2018).

In the literature, different researchers have adopted different configurations, e.g., various locations of load cells in the test. The influences of test setups on impact force measurement accuracy of RC beam under drop weight impact were investigated in the previous study (Li et al., 2020). It is found that when the load cell is embedded into drop weight, the mass distribution of drop weight causes the measured impact force to deviate from the actual

contact force acting on the beam. Therefore, for the calibration of numerical model, the load cell should be simulated as per the testing setup for a more reliable and accurate comparison of the simulation and testing results.

Conclusions

This study has reviewed previous analytical, experimental, and numerical investigations on the impact response of concrete beams. Assumptions for analytical solutions and important factors for impact tests have been discussed. This effort aims to improve understanding of impact problems with RC beams and clarify some previous findings. From the above critical review and thorough analyses and discussions, the following primary suggestions can be made:

1. For the experimental testing, the impact force should be measured by using a load cell incorporated to an impactor. The common calibration factor for the load cell under static load can be used to measure impact forces. The sampling rate of 50 kHz is appropriate to achieve reasonably accurate measurements for the reviewed RC beam sizes. The hemispherical or curved shape is suggested for the head of impactor. The reaction forces of RC beams subjected to impact loads should be measured by two load cells.
2. To derive a spring-mass model, the equivalent beam stiffness, length, and mass of an RC beam in a spring-mass model should consider the domination of local or global responses. The damping ratios for the force phase and the free vibration phase should be different.
3. For numerical investigations, the scale factors for contact mechanism in a numerical model require a careful calibration with experimental data to verify the reliability of

the contact modelling. The correlation between mesh size and erosion limit also requires careful justifications.

More researches are deemed necessary to unveil the sophisticated impact problems, such as (a) explain the mechanism of induced negative reaction forces, (b) examine the distribution of inertia force after the peak impact force, (c) proposes more reliable and robust contact models with less sensitive parameters, (d) carry out experimental test on full scale structures, and (e) propose a reliable design procedure of the impact resistance of RC beams.

Acknowledgements

The authors would like to thank the financial support from the Australian Research Council Laureate Fellowships FL180100196.

References

Abrate S (2001) Modeling of impacts on composite structures. *Composite Structures* 51(2): 129-138.

Abrate S (2005) *Impact on composite structures.* Cambridge university press.

Adhikary SD, Li B and Fujikake K (2013) Strength and behavior in shear of reinforced concrete deep beams under dynamic loading conditions. *Nuclear Engineering and Design* 259: 14-28.

Adhikary SD, Li B and Fujikake K (2015) Low Velocity Impact Response of Reinforced Concrete Beams: Experimental and Numerical Investigation. *International Journal of Protective Structures* 6(1): 81-111.

Al-Rifaie A, Guan ZW, Jones SW, et al. (2017) Lateral impact response of end-plate beam-column connections. *Engineering Structures* 151: 221-234.

Al-Rifaie A, Jones SW, Wang QY, et al. (2018) Experimental and numerical study on lateral impact response of concrete filled steel tube columns with end plate connections. *International Journal of Impact Engineering* 121: 20-34.

Alves J, Peixinho N, da Silva MT, et al. (2015) A comparative study of the viscoelastic constitutive models for frictionless contact interfaces in solids. *Mechanism and Machine Theory* 85: 172-188.

Anderson TA (2005) An investigation of SDOF models for large mass impact on sandwich composites. *Composites Part B: Engineering* 36(2): 135-142.

Anil Ö, Durucan C, Erdem RT, et al. (2016) Experimental and numerical investigation of reinforced concrete beams with variable material properties under impact loading. *Construction and Building Materials* 125: 94-104.

Bangash M (2009) *Shock, impact and explosion: structural analysis and design.* Springer Berlin.

Banthia NP, Mindess S and Bentur A (1987) Impact behaviour of concrete beams. *Materials and Structures* 20(4): 293-302.

Bednarek T and Kowalczyk P (2013) Improvement of stability conditions, accuracy and uniqueness of penalty approach in contact modeling. *Computational Mechanics* 51(6): 949-959.

Bhatti AQ and Kishi N (2011) An application of impact-response analysis on small-scale RC arch-type beams without stirrups. *Construction and Building Materials* 25(10): 3972-3976.

Bhatti AQ, Kishi N, Mikami H, et al. (2009) Elasto-plastic impact response analysis of shear-failure-type RC beams with shear rebars. *Materials & Design* 30(3): 502-510.

Biggs JM (1964) *Introduction to structural dynamics.* McGraw-Hill College.

Bischoff PH, Perry SH and Eibl J (1990) Contact force calculations with a simple spring-mass model for hard impact: A case study using polystyrene aggregate concrete. *International Journal of Impact Engineering* 9(3): 317-325.

Brannon RM and Leelavanichkul S (2009) Survey of four damage models for concrete. *Sandia National Laboratories* 32(1): 1-80.

Chaudhari S and Chakrabarti M (2012) Modeling of concrete for nonlinear analysis using finite element code ABAQUS. *International Journal of Computer Applications* 44(7): 14-18.

Chen Y and May IM (2009) Reinforced concrete members under drop-weight impacts. *Proceedings of the ICE-Structures and Buildings* 162(1): 45-56.

Cotsovos DM (2010) A simplified approach for assessing the load-carrying capacity of reinforced concrete beams under concentrated load applied at high rates. *International Journal of Impact Engineering* 37(8): 907-917.

Cui J, Hao H and Shi Y (2017) Discussion on the suitability of concrete constitutive models for high-rate response predictions of RC structures. *International Journal of Impact Engineering* 106: 202-216.

Dey V, Bonakdar A and Mobasher B (2014) Low-velocity flexural impact response of fiber-reinforced aerated concrete. *Cement and Concrete Composites* 49: 100-110.

Do TV, Pham TM and Hao H (2018) Dynamic responses and failure modes of bridge columns under vehicle collision. *Engineering Structures* 156: 243-259.

Do TV, Pham TM and Hao H (2019a) Impact Force Profile and Failure Classification of Reinforced Concrete Bridge Columns against Vehicle Impact. *Engineering Structures* 183: 443-458.

Do TV, Pham TM and Hao H (2019b) Proposed Design Procedure for Reinforced Concrete Bridge Columns against Vehicle Collisions. *Structures* 22(December): 213-229.

Dogan F, Hadavinia H, Donchev T, et al. (2012) Delamination of impacted composite structures by cohesive zone interface elements and tiebreak contact. *Central European Journal of Engineering* 2(4): 612-626.

Dragos J and Wu C (2014) Interaction between direct shear and flexural responses for blast loaded one-way reinforced concrete slabs using a finite element model. *Engineering Structures* 72: 193-202.

Erki M and Meier U (1999) Impact loading of concrete beams externally strengthened with CFRP laminates. *Journal of Composites for Construction* 3(3): 117-124.

Flores P and Ambrósio J (2010) On the contact detection for contact-impact analysis in multibody systems. *Multibody System Dynamics* 24(1): 103-122.

Flores P, Leine R and Glocker C (2010) Modeling and analysis of planar rigid multibody systems with translational clearance joints based on the non-smooth dynamics approach. *Multibody System Dynamics* 23(2): 165-190.

Foo CC, Seah LK and Chai GB (2011) A modified energy-balance model to predict low-velocity impact response for sandwich composites. *Composite Structures* 93(5): 1385-1393.

Fu H, Erki M and Seckin M (1991) Review of effects of loading rate on reinforced concrete. *Journal of Structural Engineering* 117(12): 3660-3679.

Fujikake K, Li B and Soeun S (2009) Impact response of reinforced concrete beam and its analytical evaluation. *Journal of Structural Engineering* 135(8): 938-950.

Goldston M, Remennikov A and Sheikh MN (2016) Experimental investigation of the behaviour of concrete beams reinforced with GFRP bars under static and impact loading. *Engineering Structures* 113: 220-232.

Hallquist JO (2006) LS-DYNA theory manual. *Livermore software Technology corporation*. 531.

Hao H (2015) Predictions of Structural Response to Dynamic Loads of Different Loading Rates. *International Journal of Protective Structures* 6(4): 585-606.

Hao H, Hao Y, Li J, et al. (2016) Review of the current practices in blast-resistant analysis and design of concrete structures. *Advances in Structural Engineering* 19(8): 1193-1223.

Hao H and Pham TM (2017) Performance of RC Beams with or without FRP Strengthening Subjected to Impact Loading. In: *Keynote paper in the 2nd World Congress on Civil, Structural, and Environmental Engineering (CSEE'17)*, Barcelona, Spain.

Hao Y and Hao H (2011) Numerical evaluation of the influence of aggregates on concrete compressive strength at high strain rate. *International Journal of Protective Structures* 2(2): 177-206.

Hao Y, Hao H, Jiang G, et al. (2013) Experimental confirmation of some factors influencing dynamic concrete compressive strengths in high-speed impact tests. *Cement and Concrete Research* 52: 63-70.

Hao Y, Hao H and Zhang X (2012) Numerical analysis of concrete material properties at high strain rate under direct tension. *International Journal of Impact Engineering* 39(1): 51-62.

Hazizan MA and Cantwell W (2003) The low velocity impact response of an aluminium honeycomb sandwich structure. *Composites Part B: Engineering* 34(8): 679-687.

Hughes B and Mahmood A (1984) Impact behaviour of prestressed concrete beams in flexure. *Magazine of Concrete Research* 36(128): 157-164.

Hughes G and Beeby A (1982) Investigation of the effect of impact loading on concrete beams. *Structural Engineer* 60(3): 45-52.

Huynh L, Foster S, Valipour H, et al. (2015) High strength and reactive powder concrete columns subjected to impact: Experimental investigation. *Construction and Building Materials* 78: 153-171.

Isaac P, Darby A, Ibell T, et al. (2017) Experimental investigation into the force propagation velocity due to hard impacts on reinforced concrete members. *International Journal of Impact Engineering* 100: 131-138.

ISO 6487:2015.(1987) Road Vehicles: Measurement Techniques in Impact Tests: Instrumentation.

Izi R, Konyukhov A and Schweizerhof K (2013) 3D frictionless contact problems with large load-steps based on the covariant description for higher order approximation. *Engineering Structures* 50: 107-114.

Jiang H and Chorzepa MG (2015) An effective numerical simulation methodology to predict the impact response of pre-stressed concrete members. *Engineering Failure Analysis* 55: 63-78.

Jiang H, Wang X and He S (2012) Numerical simulation of impact tests on reinforced concrete beams. *Materials & Design* 39: 111-120.

Johnson GR and Holmquist TJ (1994) An improved computational constitutive model for brittle materials. *High‐pressure science and technology—1993*. AIP Publishing, 981-984.

Johnson W (1972) *Impact strength of materials*. Edward Arnold London.

Jones N (2011) *Structural impact*. Cambridge university press.

Kishi N and Bhatti AQ (2010) An equivalent fracture energy concept for nonlinear dynamic response analysis of prototype RC girders subjected to falling-weight impact loading. *International Journal of Impact Engineering* 37(1): 103-113.

Kishi N, Khasraghy SG and Kon-No H (2011) Numerical simulation of reinforced concrete beams under consecutive impact loading. *ACI Structural Journal* 108(4): 444-452.

Kishi N and Mikami H (2012) Empirical formulas for designing reinforced concrete beams under impact loading. *ACI Structural Journal* 109(4): 509-519.

Kishi N, Mikami H, Matsuoka K, et al. (2002a) Impact behavior of shear-failure-type RC beams without shear rebar. *International Journal of Impact Engineering* 27(9): 955-968.

Kishi N, Mikami H, Matsuoka KG, et al. (2002b) Impact behavior of shear-failure-type RC beams without shear rebar. *International Journal of Impact Engineering* 27(9): 955-968.

Krauthammer T, Assadi-Lamouki A and Shanaa H (1993) Analysis of impulsively loaded reinforced concrete structural elements—II. Implementation. *Computers & Structures* 48(5): 861-871.

Krauthammer T, Bazeos N and Holmquist T (1986) Modified SDOF analysis of RC box-type structures. *Journal of Structural Engineering* 112(4): 726-744.

Lee EH (1940) The impact of a mass striking a beam. *ASME Journal of Applied Mechanics* 7: 129-138.

Lee J-Y, Shin H-O, Yoo D-Y, et al. (2018) Structural response of steel-fiber-reinforced concrete beams under various loading rates. *Engineering Structures* 156: 271-283.

Lee W-S and Lam H-F (1996) The deformation behaviour and microstructure evolution of high-strength alloy steel at high rate of strain. *Journal of Materials Processing Technology* 57(3-4): 233-240.

Li C, Qin F, Ya-Dong Z, et al. (2010) Numerical and Experimental Investigations on the blast-resistant properties of arched RC blast doors. *International Journal of Protective Structures* 1(3): 425-441.

Li H, Chen W and Hao H (2019a) Influence of drop weight geometry and interlayer on impact behavior of RC beams. *International Journal of Impact Engineering* 131: 222-237.

Li H, Chen W and Hao H (2019b) Influence of drop weight mass distribution and load cell location on impact force. In: *13th International Conference on Shock & Impact Loads on Structures*, Guangzhou, China.

Li H, Chen W and Hao H (2020) Factors influencing impact force profile and measurement accuracy in drop weight impact tests. *International Journal of Impact Engineering*. 103688.

Li H, Chen W, Pham TM, et al. (2021) Analytical and numerical studies on impact force profile of RC beam under drop weight impact. *International Journal of Impact Engineering* 147: 103743.

Li J and Hao H (2014) Numerical study of concrete spall damage to blast loads. *International Journal of Impact Engineering* 68: 41-55.

Li Z, Khennane A, Hazell PJ, et al. (2018) Performance of a hybrid GFRP-concrete beam subject to low-velocity impacts. *Composite Structures* 206: 425-438.

Lichtenfeld JA, Van Tyne CJ and Mataya MC (2006) Effect of strain rate on stress-strain behavior of alloy 309 and 304L austenitic stainless steel. *Metallurgical and Materials Transactions A* 37(1): 147-161.
Liu J and Jones N (1987) Experimental investigation of clamped beams struck transversely by a mass. *International Journal of Impact Engineering* 6(4): 303-335.
Liu T and Xiao Y (2017) Impact Behavior of CFRP-Strip–Wrapped RC Beams without Stirrups. *Journal of Composites for Construction* 21(5): 04017035.
Low HY and Hao H (2002) Reliability analysis of direct shear and flexural failure modes of RC slabs under explosive loading. *Engineering Structures* 24(2): 189-198.
LS-Dyna (2012) keyword user's manual V971. *2Livermore Technology Software Corporation, Livermore, CA*. 2994.
LSTC (2007) LS-DYNA Keyword User's Manual. *Livermore software Technology corporation*.
Lu G and Yu T (2003) *Energy absorption of structures and materials.* Elsevier.
Luccioni B, Aráoz G and Labanda N (2013a) Defining Erosion Limit for Concrete. *International Journal of Protective Structures* 4(3): 315-340.
Luccioni BM, Aráoz GF and Labanda NA (2013b) Defining erosion limit for concrete. *International Journal of Protective Structures* 4(3): 315-340.
Machado M, Moreira P, Flores P, et al. (2012) Compliant contact force models in multibody dynamics: Evolution of the Hertz contact theory. *Mechanism and Machine Theory* 53: 99-121.
Malvar LJ (1998) Review of static and dynamic properties of steel reinforcing bars. *ACI Materials Journal* 95(5): 609-614.
Malvar LJ, Crawford JE, Wesevich JW, et al. (1997) A plasticity concrete material model for DYNA3D. *International Journal of Impact Engineering* 19(9): 847-873.
Mongeau M and Sartenaer A (1995) Automatic decrease of the penalty parameter in exact penalty function methods. *European Journal of Operational Research* 83(3): 686-699.
Nour‐Omid B and Wriggers P (1987) A note on the optimum choice for penalty parameters. *Communications in Applied Numerical Methods* 3(6): 581-585.
Olsson R (2000) Mass criterion for wave controlled impact response of composite plates. *Composites Part A: Applied Science and Manufacturing* 31(8): 879-887.
Ožbolt J and Sharma A (2011) Numerical simulation of reinforced concrete beams with different shear reinforcements under dynamic impact loads. *International Journal of Impact Engineering* 38(12): 940-950.
Papadrakakis M, Papadopoulos V, Stefanou G, et al. (2016) FE Modelling of SFRC Beams under Impact Loads. In: *European Congress on Computational Methods in Applied Sciences and Engineering* (ed M. Papadrakakis VP, G. Stefanou, V. Plevris), Crete Island, Greece, pp.8640-8653.
Pham TM, Chen W, Elchalakani M, et al. (2020) Experimental Investigation on Lightweight Rubberized Concrete Beams Strengthened with BFRP Sheets Subjected to Impact Loads. *Engineering Structures* 205: 110095.
Pham TM, Do TV and Hao H (2021) Distinguished Impact Response of Hollow Reinforced Concrete Beams under Impact Loading. *ACI Special Publication* Accepted.
Pham TM and Hao H (2016) Impact behavior of FRP-strengthened RC beams without stirrups. *Journal of Composites for Construction* 20(4): 04016011.
Pham TM and Hao H (2017a) Axial impact resistance of FRP-confined concrete. *Journal of Composites for Construction* 21(2): 04016088.
Pham TM and Hao H (2017b) Behavior of fiber reinforced polymer strengthened reinforced concrete beams under static and impact loads. *International Journal of Protective Structures* 8(1): 1-22.

Pham TM and Hao H (2017c) Effect of the plastic hinge and boundary condition on the impact behaviour of RC beams. *International Journal of Impact Engineering* 102: 74-85.
Pham TM and Hao H (2017d) Plastic hinges and inertia forces in RC beams under impact loads. *International Journal of Impact Engineering* 103: 1-11.
Pham TM and Hao H (2018) Influence of global stiffness and equivalent model on prediction of impact response of RC beams. *International Journal of Impact Engineering* 113: 88-97.
Pham TM, Hao Y and Hao H (2018) Sensitivity of impact behaviour of RC beams to contact stiffness. *International Journal of Impact Engineering* 112: 155-164.
Rabczuk T and Eibl J (2006) Modelling dynamic failure of concrete with meshfree methods. *International Journal of Impact Engineering* 32(11): 1878-1897.
Remennikov AM, Kong SY and Uy B (2013) The response of axially restrained non-composite steel–concrete–steel sandwich panels due to large impact loading. *Engineering Structures* 49: 806-818.
Rhazi J, Hassaim M, Ballivy G, et al. (2002) Effects of concrete non-homogeneity on Rayleigh waves dispersion. *Magazine of Concrete Research* 54(3): 193-201.
Riedel W, Thoma K and Hiermaier S (1999) Penetration of reinforced concrete by BETA-B-500 – numerical analysis using a new macroscopic concrete model for hydrocodes. *9th International Symposium on Interaction of the Effect of Munitions with Structures.* Strausberg, Berlin, 315-322.
Ross TJ and Krawinkler H (1985) Impulsive direct shear failure in RC slabs. *Journal of Structural Engineering* 111(8): 1661-1677.
Rubinov AM, Yang XQ and Bagirov AM (2002) Penalty functions with a small penalty parameter. *Optimization Methods and Software* 17(5): 931-964.
Saatci S and Vecchio FJ (2009) Effects of shear mechanisms on impact behavior of reinforced concrete beams. *ACI Structural Journal* 106(1): 78-86.
Sharma A and Ožbolt J (2014) Influence of high loading rates on behavior of reinforced concrete beams with different aspect ratios–A numerical study. *Engineering Structures* 79: 297-308.
Shivaswamy S and Lankarani H (1997) Impact analysis of plates using quasi-static approach. *Journal of Mechanical Design* 119(3): 376-381.
Silva PF, Mesia WD, Marzougui D, et al. (2009) Performance evaluation of flexure impact resistance capacity of reinforced concrete members. *ACI Structural Journal* 106(5).
Soleimani SM and Banthia N (2014) A Novel Drop Weight Impact Setup for Testing Reinforced Concrete Beams. *Experimental Techniques* 38(3): 72-79.
Stronge WJ and Yu T (1993) *Dynamic models for structural plasticity*. Springer Science & Business Media.
Suaris W and Shah S (1981) Inertial effects in the instrumented impact testing of cementitious composites. *Cement, Concrete and Aggregates* 3(2): 77-83.
Tachibana S, Masuya H and Nakamura S (2010) Performance based design of reinforced concrete beams under impact. *Natural Hazards and Earth System Science* 10(6): 1069-1078.
Tang T and Saadatmanesh H (2003) Behavior of Concrete Beams Strengthened with Fiber-Reinforced Polymer Laminates under Impact Loading. *Journal of Composites for Construction* 7(3): 209-218.
Tang T and Saadatmanesh H (2005) Analytical and experimental studies of fiber-reinforced polymer-strengthened concrete beams under impact loading. *ACI Structural Journal* 102(1): 139-149.
Tran TT, Pham TM, Huang Z, et al. (2021) Impact Response of Fibre Reinforced Geopolymer Concrete Beams with BFRP Bars and Stirrups. *Engineering Structures* 231: 111785.

Ulzurrun GSD and Zanuy C (2017) Enhancement of impact performance of reinforced concrete beams without stirrups by adding steel fibers. *Construction and Building Materials* 145: 166-182.

Villavicencio R and Guedes Soares C (2011) Numerical modelling of the boundary conditions on beams stuck transversely by a mass. *International Journal of Impact Engineering* 38(5): 384-396.

Wang N, Mindess S and Ko K (1996) Fibre reinforced concrete beams under impact loading. *Cement and Concrete Research* 26(3): 363-376.

Wang S and Guedes Soares C (2014) Numerical study on the water impact of 3D bodies by an explicit finite element method. *Ocean Engineering* 78: 73-88.

Wang W, Wu C, Li J, et al. (2019) Behavior of ultra-high performance fiber-reinforced concrete (UHPFRC) filled steel tubular members under lateral impact loading. *International Journal of Impact Engineering* 132: 103314.

Wongmatar P, Hansapinyo C, Vimonsatit V, et al. (2018) Recommendations for Designing Reinforced Concrete Beams Against Low Velocity Impact Loads. *International Journal of Structural Stability and Dynamics*. 1850104.

Wu KQ and Yu TX (2001) Simple dynamic models of elastic–plastic structures under impact. *International Journal of Impact Engineering* 25(8): 735-754.

Wu M, Chen Z and Zhang C (2015) Determining the impact behavior of concrete beams through experimental testing and meso-scale simulation: I. Drop-weight tests. *Engineering Fracture Mechanics* 135: 94-112.

Wu M, Zhang C and Chen Z (2016) Drop-weight tests of concrete beams prestressed with unbonded tendons and meso-scale simulation. *International Journal of Impact Engineering* 93: 166-183.

Xu J, Wu C and Li Z-X (2014) Analysis of direct shear failure mode for RC slabs under external explosive loading. *International Journal of Impact Engineering* 69: 136-148.

Yan Q, Sun B, Liu X, et al. (2018) The effect of assembling location on the performance of precast concrete beam under impact load. *Advances in Structural Engineering* 21(8): 1211-1222.

Yi W-J, Zhao D-B and Kunnath SK (2016) Simplified approach for assessing shear resistance of reinforced concrete beams under impact loads. *ACI Structural Journal* 113(4): 747.

Yilmaz M, Anil Ö, Alyavuz B, et al. (2014) Load displacement behavior of concrete beam under monotonic static and low velocity impact load. *International Journal of Civil Engineering* 12(4): 488-503.

Yoo D-Y and Banthia N (2017) Size-dependent impact resistance of ultra-high-performance fiber-reinforced concrete beams. *Construction and Building Materials* 142: 363-375.

Yoo D-Y, Banthia N, Kim S-W, et al. (2015) Response of ultra-high-performance fiber-reinforced concrete beams with continuous steel reinforcement subjected to low-velocity impact loading. *Composite Structures* 126: 233-245.

Zhan T, Wang Z and Ning J (2015) Failure behaviors of reinforced concrete beams subjected to high impact loading. *Engineering Failure Analysis* 56: 233-243.

Zhao D-B, Yi W-J and Kunnath SK (2017a) Shear Mechanisms in Reinforced Concrete Beams under Impact Loading. *Journal of Structural Engineering* 143(9): 04017089.

Zhao D, Yi W and Kunnath SK (2017b) Shear Mechanisms in Reinforced Concrete Beams under Impact Loading. *Journal of Structural Engineering* 143(9): 04017089.

Zhou D and Stronge W (2006) Low velocity impact denting of HSSA lightweight sandwich panel. *International Journal of Mechanical Sciences* 48(10): 1031-1045.

Zhou X, Zhang R, Xiong R, et al. (2019) An Experimental Study of the Impact Mechanical Properties of RC Beams following Replacements of Stainless Steel Reinforcements of Equal Strength. *Advances in Materials Science and Engineering* 2019.

List of Figures

List of Tables

1 Table 1. Summary of drop-weight tests on RC beams

Reference	Impact force measure	Reaction force	Negative reaction force	Sampling rate	Data processing	Contact condition	Impactor shape
Pham and Hao (2017b)	load cell on beam	two load cells	Yes	50 kHz	-	Steel plate	hemispherical
Pham and Hao (2016)	load cell on beam	two load cells	None	50 kHz	-	Steel plate	hemispherical
Saatci and Vecchio (2009)	indirect	one load cell	None	2.4 kHz	-	Steel plate	flat
Kishi et al. (2002a)	incorporated load cell	one load cell	None	-	-	-	hemispherical
Kishi and Mikami (2012)	incorporated load cell	one load cell	-	40 kHz	moving window	direct	hemispherical
Wang et al. (1996)	incorporated load cell	no restrain and no load cell	None	100 kHz	cut off frequency of 6.2 kHZ	direct	curved
Tang and Saadatmanesh (2005)	-	one load cell	None	-	-	-	curved
Fujikake et al. (2009)	incorporated load cell	-	-	100 kHz	-	direct	hemispherical
Bhatti et al. (2009)	incorporated load cell	one load cell	None	40 kHz	-	direct	hemispherical
Banthia et al. (1987)	incorporated load cell	one load cell	None	5 Hz	-	direct	-
Hughes and Mahmood (1984)	-	one load cell	-	-	-	-	-
Zhao et al. (2017a)	incorporated load cell	one load cell	Yes	100 kHz	-	Steel plate	hemispherical
Zhan et al. (2015)	incorporated load cell	-	-	250 kHz	-	rubber pad	flat, wedge type
Wu et al. (2015)	load cell on beam	no restraint	-	100 kHz	cut off 5 kHz	pad	hemispherical
Tang and Saadatmanesh (2003)	-	restrained and load cell	None	-	-	direct	curved
Tachibana et al. (2010)	incorporated load cell	restrained and	-	20 KHz	-	direct	curved

		load cell					
Soleimani and Banthia (2014)	incorporated load cell	restrained and load cell	None	100 kHz	-	direct	curved, wedge type
Silva et al. (2009)	incorporated load cell	no load cell	-	-	-	direct	spherical ball
Liu and Xiao (2017)	incorporated load cell	restrained and load cell	None	100 kHz	cut off 6 kHz	direct	flat
Hughes and Beeby (1982)	incorporated load cell	restrained and load cell	-	-	-	various pads	spherical ball
Goldston et al. (2016)	incorporated load cell	restrained and load cell	None	50 kHz	-		direct
Bhatti and Kishi (2011)	incorporated load cell	restrained and load cell	-	40 kHz	moving window	direct	curved
Adhikary et al. (2013)	incorporated load cell	restrained	-	10 kHz-200 kHz	-	steel plate	flat

2 "-" indicates not mentioned and incorporated load cell means the load cell is fixed to the impactor.

3 Table **2.** Punching shear failure concrete structures subjected to impact loads

Reference	ID	Structural properties			Peak impact force (kN)	Failure	Dynamic shear resistance (kN)
		W (mm)	*D* (mm)	f_c (MPa)			
Do et al. (2019a)	C5	600	600	34.0	8,036	Punching shear	7,956
	C6	800	800	34.0	14,593	Punching shear	14,144
Do et al. (2018)	C14	1,200	1200	34.0	30,000	Punching shear	31,824
Pham et al. (2018)	Beam 1	150	250	46.0	1,000	Punching shear cracks	1,121
	Beam 2	150	250	52.0	1,390	Punching shear cracks	1,268
Yi et al. (2016)	BD4	150	310	41.4	1,465	Punching shear	1,242
Zhao et al. (2017a)	B-868-7.14	200	500	24.8	1,480	Punching shear	1,612
	C-868-7.14	200	500	26.3	1,735	Punching shear	1,709
	D-868-7.14	200	500	25.0	1,679	Punching shear	1,625

4